Progress In Electromagnetics Research C, Vol. 49, 1–10, 2014

UWB Monopole Antenna with Triple Band-Notched Characteristic Based on a Pair of Novel Resonators

Junhui Wang*, Zedong Wang, Yingzeng Yin, and Xianglong Liu

Abstract—In this paper, a novel microstrip-fed compact antenna with triple band-notched characteristics is presented for ultrawideband (UWB) applications. The antenna consists of a circular radiating patch, a 50 Ω microstrip feed line, a partially slotted ground plane, and a pair of modified capacitance loaded loop (MCLL) resonators. The novel resonators are symmetrically located in the vicinity of the feed line to achieve triple band-notched characteristics, such as 3.4–3.7 GHz for WiMAX, 5.15–5.825 GHz for WLAN, 7.25–8.395 GHz for X-band satellite communication. The good performance of triple notched bands, stable gain and omnidirectional radiation patterns in the operating bands make the proposed antenna a good candidate for UWB utilization.

1. INTRODUCTION

Since the Federal Communication Commission (FCC) released the frequency band of 3.1–10.6 GHz for commercial communication ultrawideband (UWB) systems, both industry and academia have exerted tremendous efforts on the UWB radio technology [1]. Antenna, as a key component of the UWB communication systems, has been investigated by many researchers. Nonetheless, antenna design still faces many challenges for UWB applications. One of the notable challenges is to avoid electromagnetic interference (EMI) with other existing narrowband services that occupy part of spectrum in the UWB band, such as 3.3–3.7 GHz for Worldwide Interoperability for Microwave Access (WiMAX) service, 5.15–5.35 & 5.725–5.825 GHz for Wireless Local Area Network (WLAN) services, and 7.25–7.745 (Down-Link) & 7.9–8.395 GHz (Up-Link) for X-band satellite communication services. To avoid the EMI problem, discrete band-stop filters are used in some UWB applications to filter the undesirable frequency bands. However, using the filters will inevitably put more complexity or constraint on the UWB systems. Therefore, a compact UWB antenna with multiple notched bands is desirable.

In order to obtain UWB antenna with band-notched characteristics, several methods have been proposed and demonstrated. One of the most popular approach is cutting different shaped slots in the radiation patch or the ground plane, such as U-shaped slot [2, 3], C-shaped slot [4, 5], L-shaped slot [6, 7], pi-shaped slot [8], and H-shaped slot [9]. Another common way is introducing parasitic strips near the radiation patch or the ground plane [10–17]. There are also other methods to realize the band-notched property. For example, in [18], a notched band around 5.5 GHz is obtained by embedding a pair of T-shaped stubs inside an elliptical slot in the radiation patch; the complementary split-ring resonator (SRR) is employed near the feed line to generate notched bands in [19]; the antenna in [20] uses a coupled C-shaped parasitic structure to obtain a band-notched function. However, most antennas of the previous works can realize only one or two notched bands. Furthermore, since each notch structure of the antennas aforementioned can achieve only one rejected band, multiple or various notch structures are required to yield multiple notched bands.

Received 4 March 2014, Accepted 25 March 2014, Scheduled 27 March 2014

* Corresponding author: Junhui Wang (xidian_wjh@163.com).

The authors are with the Laboratory of Science and Technology on Antennas and Microwaves, Xidian University, Xi'an, Shaanxi 710071, China.

In the paper, a novel microstrip-fed planar UWB antenna with triple band-notched characteristics is proposed. To realize the triple band-notched property, a novel modified capacitance loaded loop (MCLL) resonator is introduced and studied. By symmetrically placing a pair of the MCLL resonators in the vicinity of the feed line of the UWB antenna, three notched bands with central frequencies at 3.55, 5.5 and 7.8 GHz can be achieved. Moreover, compared with the notch structures mentioned in the antennas above [2–20], the MCLL resonator has triple resonant frequencies that result in the generation of three notched bands of the UWB antenna. The proposed design is simulated using the ANSYS High Frequency Structure Simulator (HFSS), a commercial 3-D full-wave electromagnetic simulation software. The antenna prototype is fabricated and measured to demonstrate the feasibility of the proposed design strategy.

2. MODIFIED CAPACITANCE LOADED LOOP RESONATOR

2.1. The Evolve Process of the Proposed Resonators

The novel MCLL resonator is introduced to achieve the triple band-notched characteristics in this paper. Figure 1 shows the evolvement process on how to obtain the proposed MCLL structure. Type I is the conventional capacitance loaded loop (CLL) resonator. Similar to the SRR resonator, the conventional CLL resonator has its own resonant frequency which can be approximated using the following expression [21]

$$f = \frac{c}{2L_{cll}\sqrt{\varepsilon}_{eff}} \tag{1}$$

where L_{cll} is the total length of the CLL structure, ε_{eff} the effective dielectric constant, and c the speed of light. Type II structure is developed from conventional Type I resonator. In the structure of Type II, the midline is attached to the ground plane by a pair of short-circuited lines. Based on the Type II structure, the midline of Type III structure is connected to a pair of folded open-circuited lines. To simplify the design of the structures, all line widths are set to 0.3 mm.

In order to analyze the frequency response characteristics of the various structures shown in Figure 1, a 50 Ω microstrip line with a pair of symmetrical resonators (Type I, II, and III) is simulated and discussed. Each pair of resonators is symmetrically placed on both sides of the microstrip line as the Type III filtering structure shown in Figure 2. All the gaps between the microtrip line and the resonators are set as 0.15 mm. Figure 3 shows the simulated results of the two-port filtering structures which are printed on the substrate with thickness of 1 mm, relative dielectric constant of 4.4 and loss tangent of 0.02. To achieve the characteristic impedance of 50 Ω, the width of the microstrip line is chosen as 1.86 mm. The simulated results indicate that the conventional Type I resonator displays only a single resonant frequency at f_3 within the UWB band (3.1–10.6 GHz), where the dimension of the resonator can be determined using the Formulas (1). Comparing the simulated results of Type II with the conventional Type I structure, it can be seen that the addition of the pair of short-circuited stubs results in the formation of a new resonance at f_1, while the original resonance at f_3 is maintained. With the addition of the open-circuited stubs in the Type III structure, another new resonant frequency at

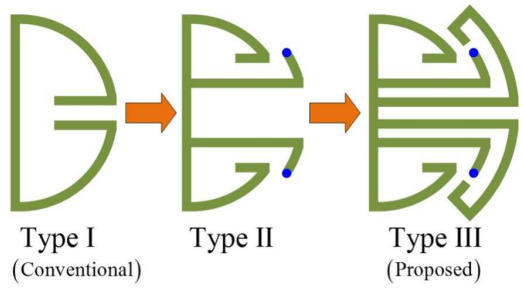

Figure 1. Evolve process of proposed structures.

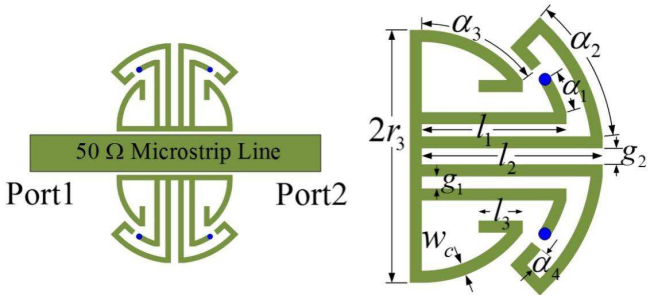

Figure 2. The two port filtering structure of Type III.

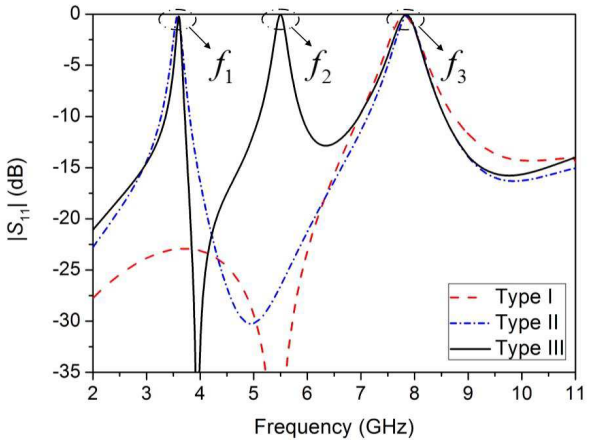

Figure 3. Simulated results of the two port filters of Type I, II and III.

f_2 is obtained. Therefore, a novel MCLL resonator with triple resonant characteristics is achieved. And the Type III filter exhibits three rejected bands with central frequencies at 3.55 (f_1), 5.5 (f_2), and 7.8 GHz (f_3). The design parameter of the MCLL resonator is as followings: $l_1 = 3.6$ mm, $g_1 = 0.3$ mm, $\alpha_1 = 15°$, $l_2 = 4.5$ mm, $g_2 = 0.4$ mm, $\alpha_2 = 40°$, $\alpha_4 = 10°$, $r_3 = 3.15$ mm, $\alpha_3 = 45.5°$, $l_3 = 1.1$ mm, $w_c = 0.3$ mm.

2.2. Equivalent Circuit Model of the Proposed Structures

For each resonant frequency response of the band-rejected filters mentioned above, the corresponding equivalent model can be demonstrated using the shunted series LC resonant circuits. Therefore, the proposed Type III filter can be equivalent to three shunt-connected series LC resonance circuits as shown in Figure 4(a). L_i and C_i ($i = 1, 2, 3$) represent values of the inductor and capacitor for each series resonant circuits. To predict the bandwidth of the series resonant circuit, the $||S_{11}|$ of the equivalent circuits can be expressed as

$$|S_{11}| = \left| \frac{1}{1 + \dfrac{2\,(j\omega L_i + 1/j\omega C_i)}{Z_0}} \right| \tag{2}$$

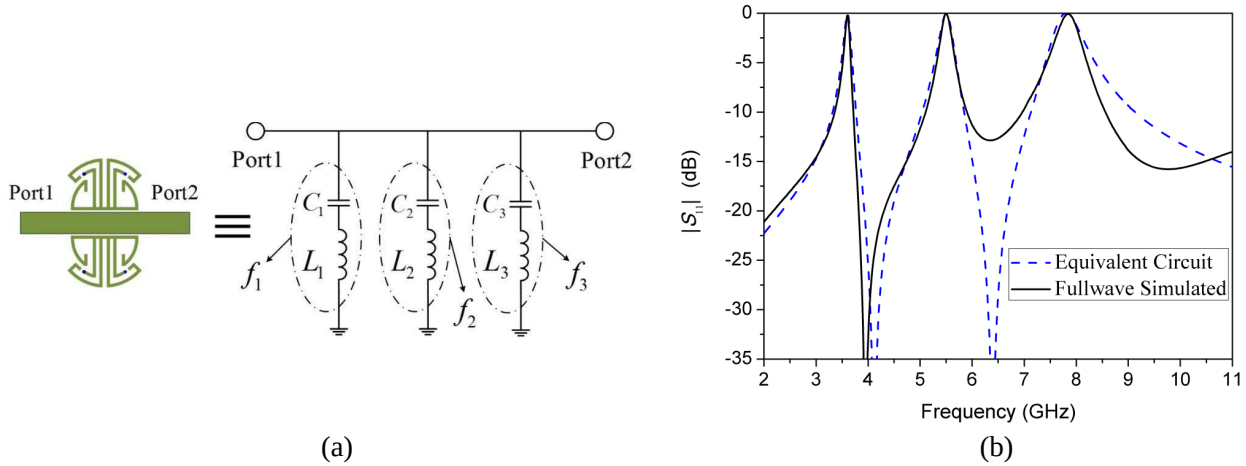

Figure 4. (a) Equivalent circuits of the Type III filter and (b) its simulated results. ($L_1 = 27.50$ nH, $C_1 = 0.071$ pF, $L_2 = 13.7$ nH, $C_2 = 0.061$ pF, $L_3 = 6.1$ nH, $C_3 = 0.068$ pF).

where Z_0 is the value of the characteristic impedance.

For a frequency near the resonant frequency (ω_0)

$$\omega = \omega_0 + \Delta\omega \tag{3}$$

$$\omega_0 = \frac{1}{\sqrt{L_i \cdot C_i}} \tag{4}$$

$$|S_{11}| = \left| \frac{1}{1 + \frac{2}{j\omega C_i Z_0}\left(1 - \omega^2 L_i C_i\right)} \right| = \left| \frac{1}{1 - \frac{2}{j\omega\omega_0^2 C_i Z_0}\left(2\omega_0\Delta\omega + \Delta\omega^2\right)} \right| \approx \left| \frac{1}{1 + j\frac{4\Delta\omega}{\omega_0^2 C_i Z_0}} \right| \tag{5}$$

Then the $-10\,\mathrm{dB}$ bandwidth of $|S_{11}|$ can be deduced using the following equations:

$$20\log|S_{11}| = -10\log\left[1 + \left(\frac{4\pi \mathrm{BW}_{-10\,\mathrm{dB}}}{\omega_0^2 C_i Z_0}\right)^2\right] = -10\,\mathrm{dB} \tag{6}$$

Thus, the $-10\,\mathrm{dB}$ bandwidth can be given by

$$\mathrm{BW}_{-10\,\mathrm{dB}} = 3\omega_0^2 C_i Z_0 / 4\pi \tag{7}$$

Using Expressions (4), (5), (6) and (7), the initial values of L_i and C_i (i = 1, 2, 3) for each series resonant circuits can be calculated respectively. After that, those values of the equivalent circuit model can be tuned and optimized using the software of ADS 2009. The simulated $|S_{11}|$ results are described in Figure 4(b), which validate the equivalent circuit model.

2.3. Key Parameter Study for the Proposed Structure

In order to analyze the parameter conveniently, the Type III structure can be replaced by the structure of Type III′ shown in Figure 5. Some key parameters of the Type III′ filtering structure are analyzed and discussed. Figure 6 shows the simulated $|S_{11}|$ results with different values α_3', while the other parameters are fixed. It can be seen that the resonant frequency f_3 decreases as α_3' increases from 35.5° to 55.5°. Figure 7 indicates the simulated results according to various angle α_2' of the arc lines. As can be seen from the simulated results, the increase of α_2' will result in decrease of resonant frequencies f_1 and f_2. It can also be found that the change of α_2' has little impact on the resonance at f_3. The simulated results with different values of α_1' are demonstrated in Figure 8. As α_1' increases from 9° to 29°, the resonant frequency f_1 shifts down dramatically while the other resonances at f_2 and f_3 change slightly. This indicates that f_1 is more susceptible to α_1'. Therefore, in order to obtain the proposed structure with desired resonant frequencies at 3.5 (f_1), 5.5 (f_2), and 7.8 GHz (f_3), the following three

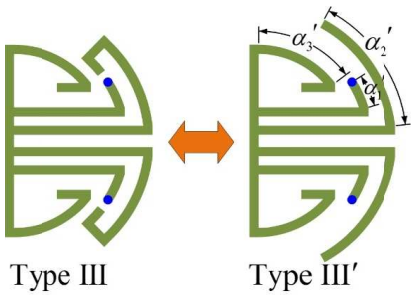

Figure 5. The equivalent structures of Type III and III′.

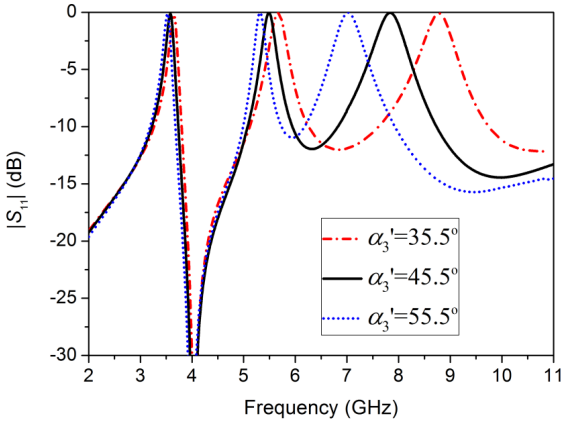

Figure 6. Simulated results of Type III′ filter with different values of parameter α_3'.

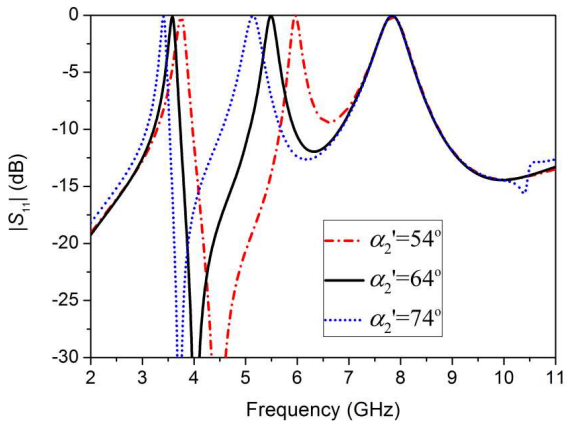

Figure 7. Simulated results of Type III′ filter with different values of parameter α_2'.

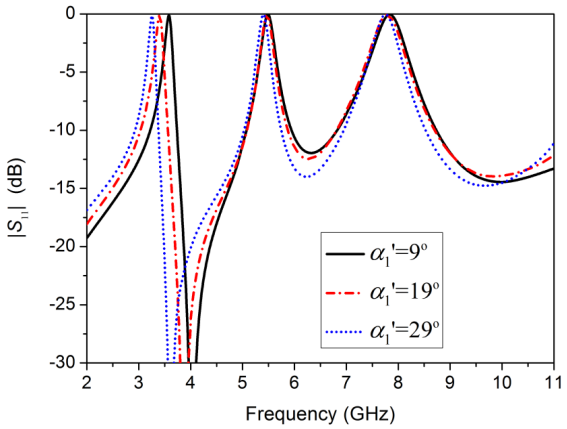

Figure 8. Simulated results of Type III' filter with different values of parameter α_1'.

steps are required. The f_3 resonance can be firstly determined to 7.8 GHz by adjusting the parameter α_3'. Then, the parameter α_2' is tuned to obtain the desired resonance at 5.5 GHz which is because the variation of α_2' does not affect f_3. The last step is to obtain the desired f_1 at 3.55 GHz by adjusting α_1', and the resonant frequencies of f_2 and f_3 will not be affected in the meantime. Finally, the resonator with triple resonant characteristics can be achieved, and the proposed Type III filter exhibits three rejected bands with central frequency around 3.55, 5.5, and 7.8 GHz.

3. TRIPLE BAND-NOTCHED ANTENNA

3.1. Geometry of the Proposed Triple Band-Notched UWB Antenna

The proposed triple band-notched monopole antenna is shown in Figure 9. The designed antenna mainly comprises a circular-shaped radiation patch, a modified ground plane and a couple of symmetrical MCLL elements. In order to enhance the impedance bandwidth, a rectangular slot underneath the feed line

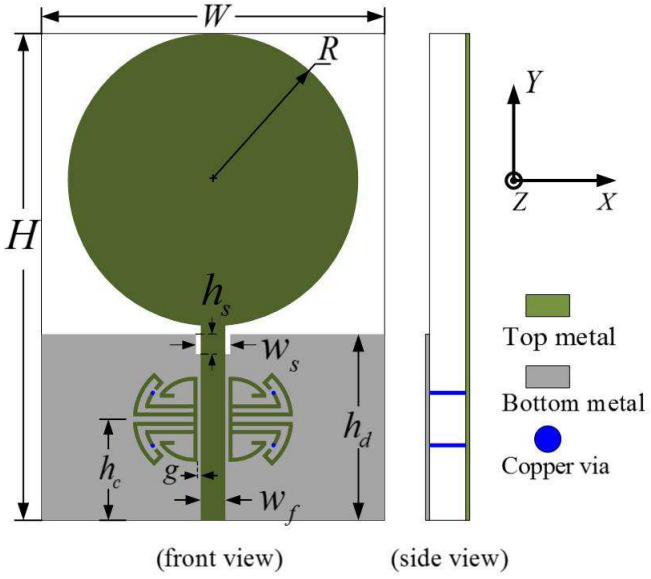

Figure 9. Geometry of the proposed antenna.

Table 1. Optimized antenna parameters.

Parameter	W	H	R	w_f	h_d	w_s	h_s
Values (mm)	26	36.6	11	1.86	14	2.6	1.5
Parameter	g	w_c	l_1	g_1	α_1	l_2	g_2
Values (mm)	0.15	0.3	3.6	0.3	14°	4.5	0.4
Parameter	α_2	α_4	r_3	α_3	l_3	h_c	
Values (mm)	40°	10°	3.15	45.5°	1.1	7.6	

Figure 10. Photos of the fabricated prototypes for proposed antenna.

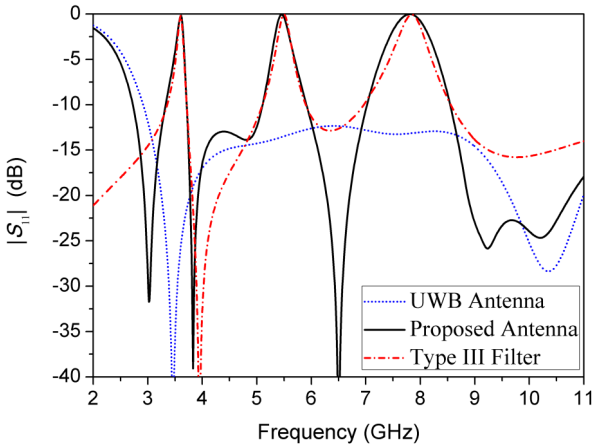

Figure 11. Simulated results of the proposed antenna.

is etched on the ground plane. Identical to the filtering structures above, the proposed antenna fed by a microstrip line is printed on an FR4 substrate with thickness of 1 mm, relative dielectric constant of 4.4 and loss tangent of 0.02. The width of the feed line is also chosen as 1.86 mm as the microstrip line of the filtering structure. In order to achieve the triple band-notched characteristics, a couple of MCLL resonators are symmetrically placed near the feed line to generate three notched bands with central frequencies at 3.55, 5.5 and 7.8 GHz. Based on the optimized dimensions given in Table 1, a prototype of triple band-notched antenna for UWB applications is designed and fabricated. Figure 10 presents a photograph of the constructed antennas.

3.2. Analysis of the Proposed Antenna

Figure 11 shows the simulated $|S_{11}|$ results against the frequency response for the proposed antenna. The UWB antenna corresponds to the proposed antenna without the MCLL resonators. And the simulated results of the proposed filter (Type III) are also shown for comparison. The UWB antenna corresponds to the proposed antenna without the MCLL resonators. From the figure it can be seen that, similar to the filter, the proposed antenna also realizes the three desired notched bands with central frequencies at 3.55, 5.5 and 7.8 GHz. To further explain the performance, the simulated surface currents distributions of the proposed antenna at three resonant frequencies are shown in Figure 12. As shown in Figure 12(a), a significant amount of current at 3.55 GHz is distributed on the additional pair of short-circuited stubs of the MCLL resonators. It can be seen that most of the input energy is coupled from the feed line to the resonators, and then flows to the ground plane through the pair of shorted lines, thus generating the notch resonance at f_1. As can be seen in Figures 12(b) and (c), the current distribution at 5.5 GHz is mainly concentrated on the pair of open-circuited stubs, while the current at 7.8 GHz is mainly distributed on the conventional CLL structures of the proposed MCLL resonators. These structures capture and store most of the input energy at the resonant frequencies f_2 and f_3,

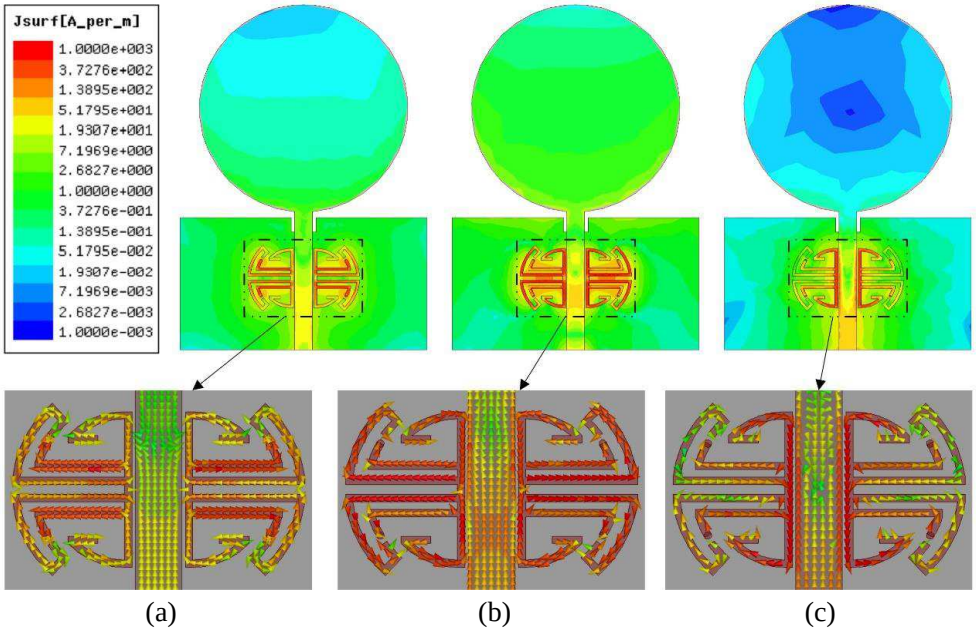

Figure 12. Simulated current distribution of the proposed antenna at three resonant frequencies of (a) 3.55 GHz, (b) 5.5 GHz, and (c) 7.8 GHz.

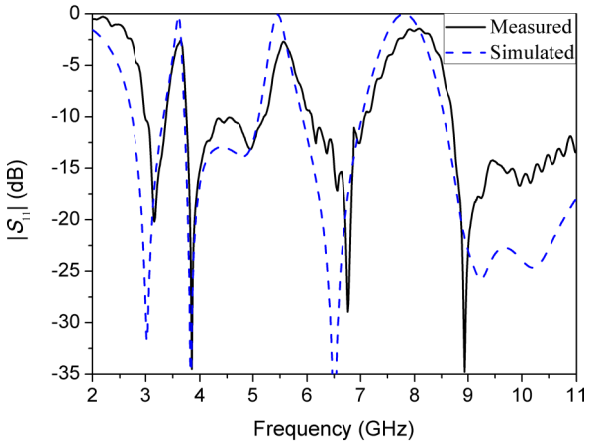

Figure 13. Measured $|S_{11}|$ results of the proposed antenna.

which results in another two notch properties. Therefore, by employing the proposed MCLL resonators, the UWB antenna with triple band-notched characteristics is achieved.

4. MEASURED RESULTS AND DISCUSSION

Based on the optimized parameters of the proposed triple band-notched UWB antenna, an antenna prototype was successfully fabricated and measured. Figure 13 displays the measured and simulated $|S_{11}|$ results of the designed antenna. It can be observed that the designed antenna exhibits three rejected bands of 3.36–3.75, 5.15–6.0, and 7.07–8.7 GHz, while achieving a wideband performance from 3 to 11 GHz for $|S_{11}| < -10$ dB. The discrepancy between measured and simulated results is probably owing to the fluctuation of dielectric constant or tolerance in manufacturing.

The measured radiation patterns in the E- (xy-) and H- (xz-) plane at 3, 4.5, 6.5 and 9.5 GHz are plotted in Figure 14. It can be seen that the proposed antenna has a nearly omnidirectional radiation

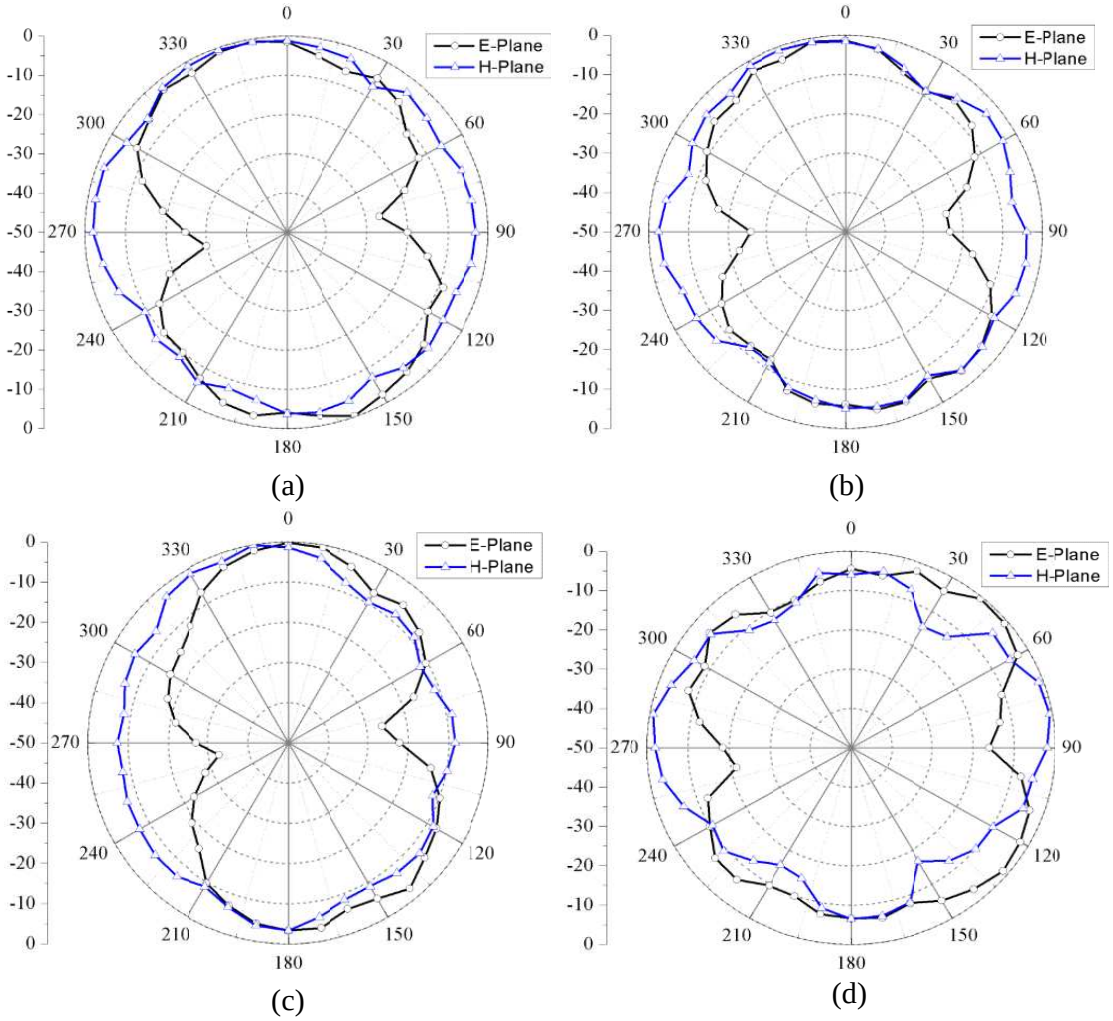

Figure 14. Measured radiation E- and H-plane radiation pattern of the proposed antenna at (a) 3, (b) 4.5, (c) 6.5, and (d) 9.5 GHz.

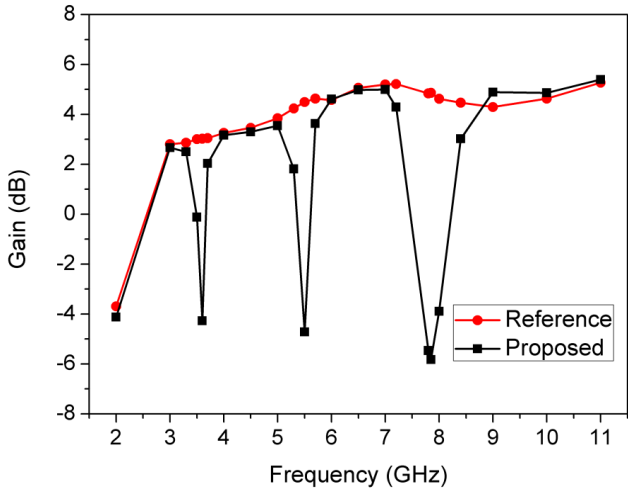

Figure 15. Measured gains of the proposed antenna.

pattern in the H-plane and a dipole-like radiation pattern in the E-plane. The measured peak gains from 3 to 11 GHz are shown in Figure 15. As illustrated in the figure, the gain decreases sharply in the vicinity of 3.55, 5.5 and 7.8 GHz. Outside the notched bands, antenna gains with variation of less than 3 dB are achieved, indicating stable gain performance across the operating bands.

5. CONCLUSION

This study presents a novel compact microstrip-fed printed monopole UWB antenna with triple band-notched characteristics. A novel MCLL resonator is introduced to realize the triple band-notched feature in this paper. By adjusting the key parameters of the resonators that are placed in mirror with each other along the feed line, the desired rejected bands can be achieved. Furthermore, employing the resonators near the feed line does not perturb the radiating performance of the UWB antenna except three notched bands, which is the distinguishing feature of the proposed method to generate the band-notched characteristics. Moreover, the simple structure, compact size and excellent performance make the proposed antenna a good candidate for various UWB applications.

REFERENCES

1. Federal Communication's Commission, "Revision of Part 15 of the commission's rules regarding ultra-wideband transmission systems, first note and order," ET-Docket 98-153, Washington, DC, 2002.
2. Kang, X. L., H. Zhang, Z. R. Li, Q. X. Guo, X. Q. Zhang, J. H. Wang, and Y. Q. Yang, "A band-notched UWB printed half elliptical ring monopole antenna," *Progress In Electromagnetics Research C*, Vol. 35, 23–33, 2013.
3. Mohammadi, S., J. Nourinia, C. Ghobadi, and M. Majidzadeh, "Compact CPW-fed rotated square-shaped patch slot antenna with band-notched function for UWB applications," *Electron. Lett.*, Vol. 47, No. 24, 1307–1309, 2011.
4. Li, C. M. and L. H. Ye, "Improved dual band-notched UWB slot antenna with controllable notched bandwidths," *Progress In Electromagnetics Research*, Vol. 115, 477–493, 2011.
5. Zheng, Z. A., Q. X. Chu, and Z. H. Tu, "Compact band-rejected ultrawideband slot antennas inserting with and resonators," *IEEE Trans. Antennas Propag.*, Vol. 59, No. 2, 390–397, 2011.
6. Tilanthe, P., P. C. Sharma, and T. K. Bandopadhyay, "A monopole microstrip antenna with enhanced dual band rejection for UWB applications," *Progress In Electromagnetics Research B*, Vol. 38, 315–331, 2012.
7. Nguyen, D. T., D. H. Lee, and H. C. Park, "Very compact printed triple band-notched UWB antenna with quarter-wavelength slots," *IEEE Antennas Wireless Propag. Lett.*, Vol. 11, 411–414, 2012.
8. Zhao, Y. L., Y. C. Jiao, G. Zhao, L. Zhang, Y. Song, and Z. B. Wong, "Compact planar monopole UWB antenna with band-notched characteristic," *Microw. Opt. Technol. Lett.*, Vol. 50, 2656–2658, 2008.
9. Deng, J. Y., Y. Z. Yin, S. G. Zhou, and Q. Z. Liu, "Compact ultrawideband antenna with tri-band notched characteristic," *Electron. Lett.*, Vol. 44, No. 21, 1231–1233, 2008.
10. Li, C. M. and L. H. Ye, "Improved dual band-notched UWB slot antenna with controllable notched bandwidths," *Progress In Electromagnetics Research*, Vol. 115, 477–493, 2011.
11. Zhu, F., S. Gao, A. T. S. Ho, C. H. See, R. A. Abd-Alhameed, J. Li, and J. Xu, "Design and analysis of planar ultra-wideband antenna with dual band-notched function," *Progress In Electromagnetics Research*, Vol. 127, 523–536, 2012.
12. Mandal, T. and D. Santanu, "An optimal design of CPW-fed UWB aperture antennas with WIMAX/WLAN notched band characteristics," *Progress In Electromagnetics Research C*, Vol. 35, 161–175, 2013.
13. Li, B., J. S. Hong, and B. Z. Wang, "Switched band-notched UWB/dual-band WLAN slot antenna with inverted S-shaped slots," *IEEE Antennas Wireless Propag. Lett.*, Vol. 11, 572–575, 2012.

14. Chen, W. S. and K. Y. Ku, "Band-rejected design of the printed open slot antenna for WLAN/WiMAX operation," *IEEE Trans. Antennas Propag.*, Vol. 56, No. 4, 1163–1169, 2008.
15. Azim, R., M. T. Islam, and A. T. Mobashsher, "Design of a dual band-notch UWB slot antenna by means of simple parasitic slits," *IEEE Antennas Wireless Propag. Lett.*, Vol. 12, 1412–1415, 2013.
16. Naser-Moghadasi, M., R. A. Sadeghzadeh, T. Sedghi, T. Aribi, and B. S. Virdee, "UWB CPW-fed fractal patch antenna with band-notched function employing folded T-shaped element," *IEEE Antennas Wireless Propag. Lett.*, Vol. 12, 504–507, 2013.
17. Abbosh, A. M. and M. E. Bialkowski, "Design of UWB planar band-notched antenna using parasitic elements," *IEEE Trans. Antennas Propag.*, Vol. 57, No. 3, 796–799, 2009.
18. Hong, C. Y., C. W. Ling, I. Y. Tarn, and S. J. Chung, "Design of a planar ultrawideband antenna with a new band-notch structure," *IEEE Trans. Antennas Propag.*, Vol. 55, No. 12, 3391–3397, 2007.
19. Sung, Y., "UWB monopole antenna with two notched bands based on the folded stepped impedance resonator," *IEEE Antennas Wireless Propag. Lett.*, Vol. 11, 500–502, 2012.
20. Ojaroudi, M. and N. Ojaroudi, "Ultra-wideband small rectangular slot antenna with variable band-stop function," *IEEE Trans. Antennas Propag.*, Vol. 62, No. 1, 490–494, 2014.
21. Lin, C. C., P. Jin, and R. W. Ziolkowski, "Single, dual and tri-band-notched ultrawideband (UWB) antennas using capacitively loaded loop (CLL) resonators," *IEEE Trans. Antennas Propag.*, Vol. 60, No. 1, 102–109, 2012.